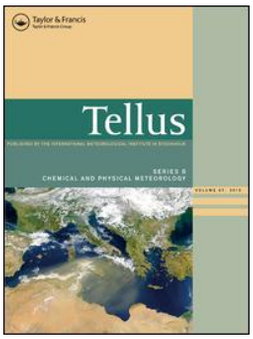

Tellus B: Chemical and Physical Meteorology

ISSN: (Print) 1600-0889 (Online) Journal homepage: https://www.tandfonline.com/loi/zelb20

Emission factors of CO_2, CO and CH_4 from Sumatran peatland fires in 2013 based on shipboard measurements

Hideki Nara, Hiroshi Tanimoto, Yasunori Tohjima, Hitoshi Mukai, Yukihiro Nojiri & Toshinobu Machida

To cite this article: Hideki Nara, Hiroshi Tanimoto, Yasunori Tohjima, Hitoshi Mukai, Yukihiro Nojiri & Toshinobu Machida (2017) Emission factors of CO_2, CO and CH_4 from Sumatran peatland fires in 2013 based on shipboard measurements, Tellus B: Chemical and Physical Meteorology, 69:1, 1399047, DOI: 10.1080/16000889.2017.1399047

To link to this article: https://doi.org/10.1080/16000889.2017.1399047

Tellus SERIES B CHEMICAL AND PHYSICAL METEOROLOGY
PUBLISHED BY THE INTERNATIONAL METEOROLOGICAL INSTITUTE IN STOCKHOLM

Emission factors of CO_2, CO and CH_4 from Sumatran peatland fires in 2013 based on shipboard measurements

By HIDEKI NARA*, HIROSHI TANIMOTO, YASUNORI TOHJIMA, HITOSHI MUKAI, YUKIHIRO NOJIRI and TOSHINOBU MACHIDA, *Center for Global Environmental Research, National Institute for Environmental Studies, Tsukuba, Japan*

(Manuscript received 24 May 2017; in final form 25 October 2017)

ABSTRACT

We observed prominent CO enhancements with simultaneous enhancements of CO_2 and CH_4 around the Malay Peninsula in South-East Asia from mid-June to mid-August 2013 based on systematic shipboard observations. We identified 18 episodes of CO enhancement during the period, which were responsible for the largest positive anomaly of CO observed in the areas of off the eastern coast of Peninsular Malaysia and in the Straits of Malacca between 2007 and 2013 based on shipboard observations. Satellite data revealed that the CO enhancements resulted mainly from the emissions from large-scale biomass burning in north-central Sumatra. We characterized five biomass burning peaks with strong fire emission signatures based on the relationship between CO_2 and CO. From these peaks, we estimated the average emission factors (EFs) for CO_2, CO and CH_4 from the fires in the study area. The estimated average EFs for CO_2 and CO agreed well with those predicted by version 4.1s of the Global Fire Emissions Database (GFED4.1s) using the recommended EF values, but the CH_4 EF differed substantially, suggesting high uncertainty of the CH_4 EF for peat in GFED4.1s. We estimated the typical EF values for peat fires based on the average EF values from the present study. The estimated typical EF values were 1663 ± 54 g/kg for CO_2, 205 ± 23 g/kg for CO and 7.6 ± 1.6 g/kg for CH_4. Despite the lack of a clear difference for CO_2 and CO, our estimated typical EF of CH_4 was less than half of the GFED4.1s-recommended EF and was comparable to previously reported EF values for Borneo peat. These results suggest a significant overestimation of the EF of CH_4 for peat fires in GFED4.1s; using the present values would greatly decrease the estimated contribution of Equatorial Asia to global fire emissions of CH_4, especially in drought years.

Keywords: peat, emission factor, methane, carbon monoxide, Indonesia, shipboard observation

1. Introduction

Biomass burning releases large amounts of the carbon stored in plant biomass and soils over time into the atmosphere in the form of gases and particulate matter. This emission affects atmospheric chemistry and climate systems at local, regional and even global scales (e.g. Crutzen and Andreae, 1990), as well as local vegetation and ecosystem dynamics (e.g. Bond and Keeley, 2005). Annual global carbon emissions from fires between 1997 and 2009 averaged approximately 2 Pg C yr^{-1}, with the annual value ranging between 1 Pg C yr^{-1} and 3 Pg C yr^{-1} (van der Werf et al., 2010). More than half of the emissions occurred in the tropics of Africa (28 and 24% from the southern and northern tropics, respectively), followed by southern hemispheric South America (13%). Despite accounting for only 2.5% of the average annual global burned area, Equatorial Asia: Malaysia, Indonesia and Papua New Guinea, is the fourth largest emitter of carbon from fires, contributing about 10% of the total. This emphasizes the importance of this region to global carbon emissions from fires.

In Equatorial Asia, large-scale biomass burning has mostly occurred in Indonesia, with fire activity increasing during the last several decades (Schultz et al., 2008; van der Werf et al., 2008; Field et al., 2009), in contrast with a decreasing global trend (Marlon et al., 2009; Wang et al., 2010; 2017). For example, Field et al. (2009) reconstructed the fire activity before the beginning of the period of global fire observation by satellite using the visibility reports from several airports located in Indonesia. These investigators showed that large-scale biomass burning in Sumatra and Borneo accompanied severe drought induced by El Niño, often boosted by a positive Indian Ocean dipole mode (IOD), since the land-use change associated with

*Corresponding author. e-mail: nara.hideki@nies.go.jp

Citation: Tellus B: 2017, **69**, 1399047, https://doi.org/10.1080/16000889.2017.1399047

rapid population growth began in the 1960s for Sumatra and in the 1980s for Borneo. Past studies revealed that the occurrence of the large-scale biomass burning was strongly connected with the conversion of intact peat swamp forests because the logging, drainage and degradation of peat swamp forests associated with the land-use change make the dry peat soils highly susceptible to fire (Siegert et al., 2001; Page et al., 2002; Field and Shen, 2008; Miettinen, Hooijer, Wang, et al., 2012). Owing to the high carbon content and fuel loading, peat soils burned by fires that escaped during conventional burning for land management produce a larger amount of carbon in the form of gases and aerosols than other vegetation fires, thereby significantly affecting the spatial and temporal distribution of greenhouse gases (Langenfelds et al., 2002; Page et al., 2002; van der Werf et al., 2004; Zeng et al., 2005), reactive gases (Logan et al., 2008; Chandra et al., 2009; Worden et al., 2013) and aerosols (Marlier et al., 2013; Gaveau et al., 2014).

In Sumatra and Borneo, deforestation of peat swamp forests has been accelerating substantially since 1990 due to increased pressure on peat swamp forest for further development of oil palm and timber plantations that will promote socio-economic development (Miettinen, Hooijer, Shi, et al., 2012; Miettinen et al., 2012, 2016; Margono et al., 2014). Past studies reported that land management and subsequent development after deforestation differed between Sumatra and Borneo, leading to different fire regimes in these regions (i.e. different spatial and temporal patterns for the occurrence of fire, and different fire intensity). van der Werf et al. (2008) reported that carbon emissions from Sumatran fires from 2000 to 2006 were nearly constant, though with a slight increasing trend that was independent of the occurrence of El Niño; in contrast, Borneo showed an abrupt increase in drought years. Miettinen et al. (2011) examined the fire activity in Equatorial Asia during La Niña (2008, wet year) and El Niño (2009, dry year) conditions. These investigators showed that fires were concentrated in the peatlands of Sumatra and Borneo occurring mostly in each drought period of Sumatra and Borneo for both the dry and wet years, with greater fire activity in the dry year. Based on the comparison of the fire activity observed in Sumatra and Borneo between the dry and wet years, these investigators revealed that Sumatran fires were predominantly large-scale land clearance fires in intensely managed peatland, whereas Bornean fires were predominantly large-scale wildfires in the dry year (2009), with little fire activity in the wet year (2008). These studies showed that differences in land management and in development of the peat swamp forests have significantly influenced the fire regimes in Sumatra and Borneo depending on weather patterns.

Gaveau et al. (2014) reported an intense peatland fire that occurred in the province of Riau, Sumatra, experiencing anomalously dry conditions during a week in June 2013, despite the absence of El Niño and a positive IOD. Although the burned area was confined to a limited area of deforested peatland, strong emissions of greenhouse gases from this fire significantly affected the average annual emissions from Indonesia, corresponding to between 5 and 10% of the total annual emissions (CO_2 equivalent) due to the combustion of peat soil. These results suggested the importance of peatland fires from Sumatra to regional anthropogenic emissions depending on the local rainfall patterns in conjunction with ongoing peatland development.

From mid-June to mid-August 2013, we detected large enhancements of several trace gases around the Malay Peninsula during systematic shipboard observations. In this study, we present observational evidence that the emissions from the peatland fires that occurred mostly in Riau province in central Sumatra in 2013, as reported by Gaveau et al. (2014), were mainly responsible for the observed enhancements by analyzing the shipboard observation data in conjunction with the satellite images of CO column distribution. We then estimated the emission factors (EF values) for CO_2, CO and CH_4 for peatland fires based on a combination of the shipboard observations and version 4.1s of the Global Fire Emissions Database (GFED-4.1s) and examined the optimal EF values for the peat for use in GFED4.1s. Our results provide a better understanding of the impact of the intense Sumatran peatland fire that occurred in the northern summer of 2013, a non-drought year, complementing a previous study by Gaveau et al. (2014).

2. Methods

2.1. *Shipboard observation*

In collaboration with two maritime shipping companies, the National Institute for Environmental Studies (NIES) has performed atmospheric monitoring of chemically and radiatively important gases over the Pacific Ocean under the NIES Volunteer Observing Ship (VOS) programme, which has been operated by the Center for Global Environmental Research of the NIES since 1992 (Nara, Tanimoto, Nojiri, Mukai, Machida, et al., 2011; Terao et al., 2011). The NIES-VOS programme first covered the remote Pacific atmosphere with help from commercial cargo vessels that were sailing between Japan and the United States, but also included vessels sailing between Japan and Australia and New Zealand, with the goal of observing background atmospheric levels of various gases to improve our understanding of the global-scale variations of greenhouse gases and other climatically important trace gases (Nara, Tanimoto, Nojiri, Mukai, Zeng, et al., 2011; Terao et al., 2011; Tohjima et al., 2012, 2015).

In September 2007, the NIES-VOS programme was augmented to allow observation of various trace gases in the anthropogenically impacted atmosphere of the South-East Asia region, showing remarkable economic growth (Nara, Tanimoto, Nojiri, Mukai, Machida, et al., 2011; Nara et al., 2014). Two commercial cargo vessels were used to support systematic atmospheric monitoring: the motor vessel (M/V) *Fujitrans World* (owned by the Kagoshima Senpaku Kaisha, Ltd.,

Kagoshima, Japan) was mainly used to obtain *in situ* measurements of CO_2, CO and O_3 using non-dispersive and gas filter correlation infrared analyzers and an ultraviolet absorption analyzer, respectively. Starting in September 2009, a wavelength-scanned cavity ring-down spectrometer was employed to provide simultaneous measurements of CO_2 and CH_4. The second VOS ship, the M/V *Trans Future 1* (owned by the Toyofuji Shipping Co. Ltd., Aichi, Japan), was used as backup ship that obtained CO_2, CH_4, CO and O_3 measurements using the same instruments as those on the M/V *Fujitrans World*. The design and performance of our *in situ* measurement systems were described in detail elsewhere (Nara, Tanimoto, Nojiri, Mukai, Machida, et al., 2011; Nara et al., 2014). The VOS ships travelled regularly between Japan and South-East Asia, with berths in Osaka, Yokohama and Nagoya (Japan); Hong Kong (China); Laem Chabang (Thailand); Singapore (Singapore); Port Klang, Kuching and Kota Kinabalu (Malaysia); Jakarta (Indonesia); and Muara (Brunei) at four-week intervals (Figure 1). These ships sail on the same shipping route during the southbound travel from Japan to Jakarta, with a time difference of about 1 week, with the M/V *Trans Future 1* sailing ahead of the M/V *Fujitrans World*, but they take different routes during the northbound travel from Jakarta to Japan: the *Fujitrans World* takes the Asia route (orange line in Figure 1) and the *Trans Future 1* takes the Borneo route (red line).

The air samples were rarely influenced by the ship's exhaust during sailing at a cruising speed of approximately 20 knots, but we tested for contamination from the exhaust by examining the variations in the dry mole fractions of CO_2 and O_3 before analyzing the data: when the data showed an abrupt CO_2 increase and O_3 decrease, we rejected the data as contaminated. At a speed of less than 5 knots, we eliminated the data to prevent possible contamination by the ship's exhaust. Unless otherwise noted, we have reported the CO data as the 1-h mean value less than 3500 ppb of upper detection limit due to the instrumental settings. We do not discuss the O_3 data in this study because our analysis focuses on the direct source emissions of CO_2, CO and CH_4.

2.2. *Satellite observations*

We used satellite observations from the Moderate Resolution Imaging Spectroradiometer (MODIS) sensors on board the Terra and Aqua satellites to examine the spatial and temporal variation of active fire locations and of fire intensity in Equatorial Asia. The Terra and Aqua satellites were launched in December 1999 and May 2002, respectively. These satellites are in sun-synchronous polar orbits; Terra crosses the equator at a local time of 10:30 AM and PM, and Aqua crosses at 1:30 AM and PM. The MODIS sensors measure radiance and reflectance in 36 spectral channels that range in wavelength from 0.4 to 14.4 μm, with a cross-track swath of 2330 km by 10 km along the track at nadir.

Active fires were detected with a 1-km spatial resolution using a contextual algorithm based on the thermal difference between the brightness temperatures measured by the 4- and 11-μm channels; the algorithm is based on the property of black-body radiation described by Planck's radiation law

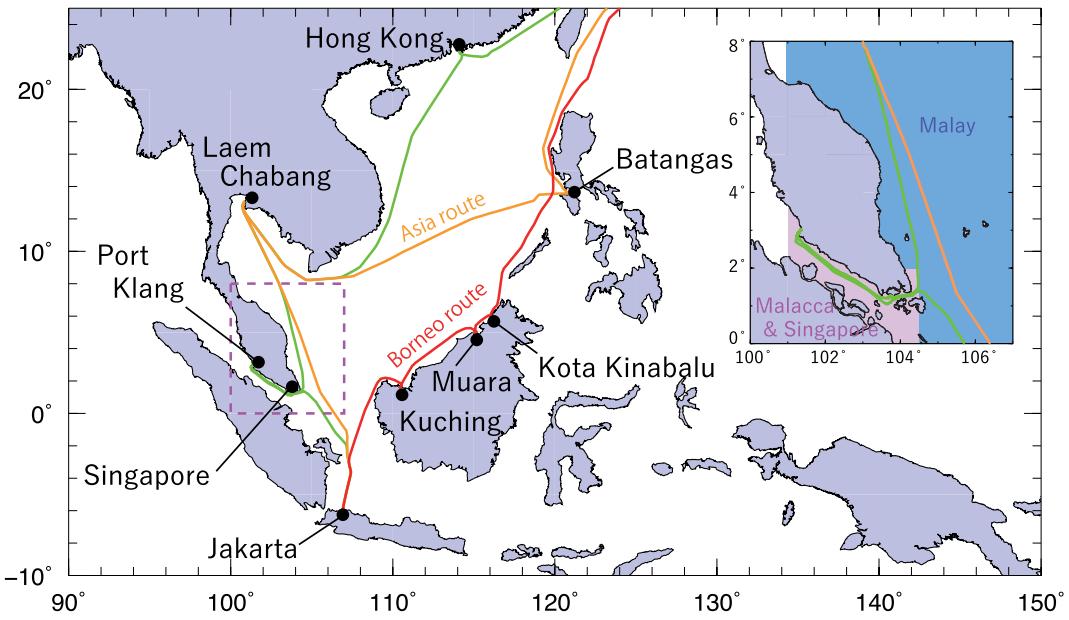

Fig. 1. The shipping route of the VOS ships in South-East Asia: southbound route (Japan to Indonesia; green); northbound Asia and Borneo routes (Indonesia–Japan; orange and red). The area surrounded by the dashed square around Peninsula Malaysia was divided into two regions for the analysis, as shown in the inset (Malay area, blue; Malacca and Singapore area, magenta).

(Kaufman et al., 1998; Giglio et al., 2003). In the fire detection processing, fire radiative power (FRP) is obtained empirically by relating it to the differences in the brightness temperature in the 4-μm channel between the fire pixel and the neighbouring non-fire background pixels. FRP is a good proxy for fire intensity, as it is linearly related to biomass combustion rates; the fire radiative energy integrating FRP over a vegetation fire is linearly related to the total mass of fuel biomass that is combusted (Wooster, 2002; Wooster et al., 2005; Giglio et al., 2006; Ichoku et al., 2008). We used the MODIS global monthly fire location product (MCD14ML, collection 5.1), which combines the Terra and Aqua MODIS Level 2 MOD14/MYD14 active fire products. The MCD14ML data contains the geographic location of each active fire, as well as other information such as the date, brightness temperatures at 4 and 11 μm, FRP, and the confidence of the fire detection. In this study, we only used active fire information with detection confidence levels greater than 30% from both the Aqua and the Terra satellites.

We also used satellite CO observation data from the Atmospheric Infrared Sounder (AIRS) instrument aboard the Aqua satellite. AIRS is a grating spectrometer with 2378 channels that cover the spectral range from 3.7 to 16 μm (Aumann et al., 2003). CO retrievals were archived at 4.7 μm even under cloudy conditions in conjunction with data from the advanced microwave sounding unit, which has a peak sensitivity at 500 hPa (Susskind et al., 2003, 2011; McMillan et al., 2005, 2011). Owing to its cross-track scanning swath width of 1650 km and spatial resolution of 45 km at nadir, daily global coverage was approximately 70%. In this study, we used the version-6 level-3 CO retrieval data from the AIRX3STD.006 and AIRX3STM.006 products to examine the daily and monthly total column distribution of CO.

2.3. *Emission inventory*

We used a global fire emissions inventory, GFED4.1s, which provides global estimates of emissions of gases and particulate matter from biomass burning based on satellite observations at a spatial resolution of 0.25° latitude by 0.25° longitude (Giglio et al., 2013). GFED4.1s, an updated version of GFED3 (van der Werf et al., 2010), currently includes the burned area, carbon and dry matter emission, and fractional contribution of total burned area for different fire types, with daily temporal resolution after operation of the MODIS sensor from 2000 to 2015. The burned area data were derived from the 500-m burned area products based on the MODIS direct broadcast burned area mapping algorithm using the burn-sensitive vegetation index calculated from the observed surface reflectance, with supplemental indirect estimation; this product relies on the climatological relationship between active fire counts and the corresponding burned area (Giglio et al., 2009, 2013). The burned area associated with active fires that were omitted in the burned area products by the direct-broadcast burned area mapping algorithm was complemented based on the algorithm of Randerson et al. (2012) for detecting the area burned by small fires. GFED4.1s provides fractional contributions of six different fire types: grassland and savannah fires, boreal forest fires, temperate forest fires, tropical forest fires in areas of deforestation and degradation, peat fires, and agricultural waste burning. These contributions were estimated according to the fraction of tree cover based on the 250-m MODIS collection-5 vegetation continuous field products and land cover type based on the 500-m MODIS collection-5 global land cover type product using the algorithm developed by Friedl et al. (2010). The carbon and dry matter emissions are simulated by the improved Carnegie-Ames-Stanford Approach biogeochemical model developed for GFED, which is driven by meteorological data and remotely sensed information (mainly from MODIS) on land surface reflectance as well as the above-mentioned burned area information (van der Werf et al., 2010). To calculate the emissions of trace gases and particulate matter from the dry matter emission, application of EF values based on the data from reports of Yokelson et al., (1997), Andreae and Merlet (2001), Christian et al. (2003), and Akagi et al. (2011) are recommended for use with the GFED4.1s.

3. Results and discussion

3.1. *Analysis of the CO enhancements*

From mid-June to mid-August 2013, simultaneous enhancements of CO_2, CO and CH_4 were observed around peninsular Malaysia along the routes of the VOS ships (Figure 2). The CO enhancements were most prominent, with 18 episodes of CO enhancement detected by visual inspection of the data. The largest CO enhancements were observed in June, with CO dry mole fractions that often exceeded the upper limit of the gas filter correlation infrared analyzer's operating range (>3500 ppb) off the eastern coast of Peninsular Malaysia and in the Straits of Malacca. In July and August, higher CO enhancements were still observed in the Straits of Malacca while lesser enhancements were observed off the eastern coast of Peninsular Malaysia.

To investigate the regional impact of the observed CO enhancements, we examined the area mean CO dry mole fractions observed in the Malay and Malacca and Singapore areas, which represent the sea off the eastern coast of Peninsular Malaysia and the sea off the coast of Singapore plus the Straits of Malacca, respectively, from the beginning of the VOS monitoring (September 2007) to December 2013 (Figures 1 and 3). The average total numbers of 1-h-mean CO data collected in the Malay and the Malacca and Singapore areas for each month resulting from the sailing along the southbound route and the northbound Asia route by the two VOS ships were 57 ± 27 (mean ± standard deviation) and 45 ± 18, respectively. Despite

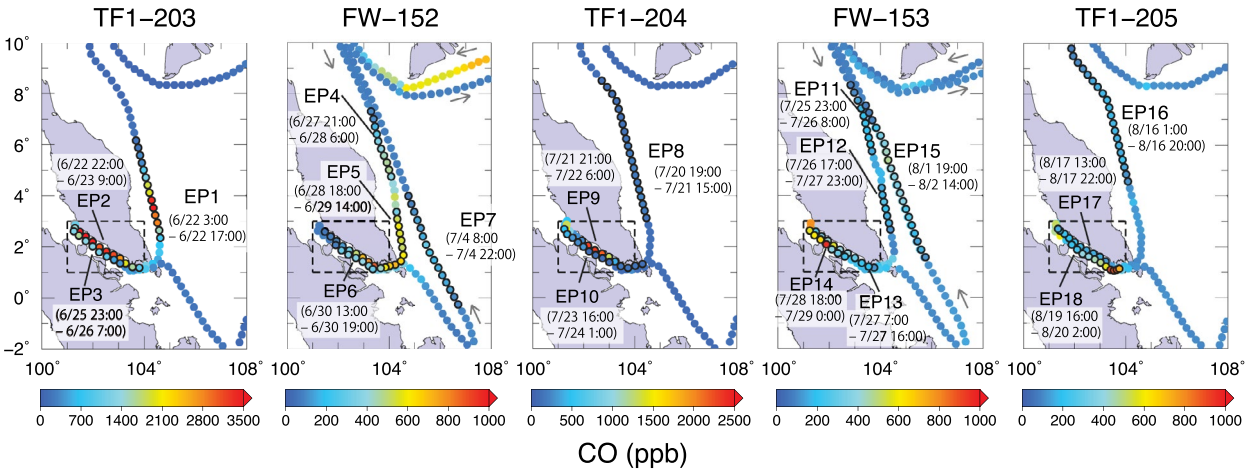

Fig. 2. CO distribution around Malay Peninsula observed by the two VOS ships during the period from mid-June to mid-August 2013. The CO distribution is shown separately for each voyage (TF1, M/V *Trans Future 1*; FW, M/V *Fujitrans World*), and the dry mole fractions of CO are plotted along the shipping route. The CO enhancement episodes are numbered individually, and CO data during the episodes are represented by black-rimmed dots, with the episode duration presented below the episode number.

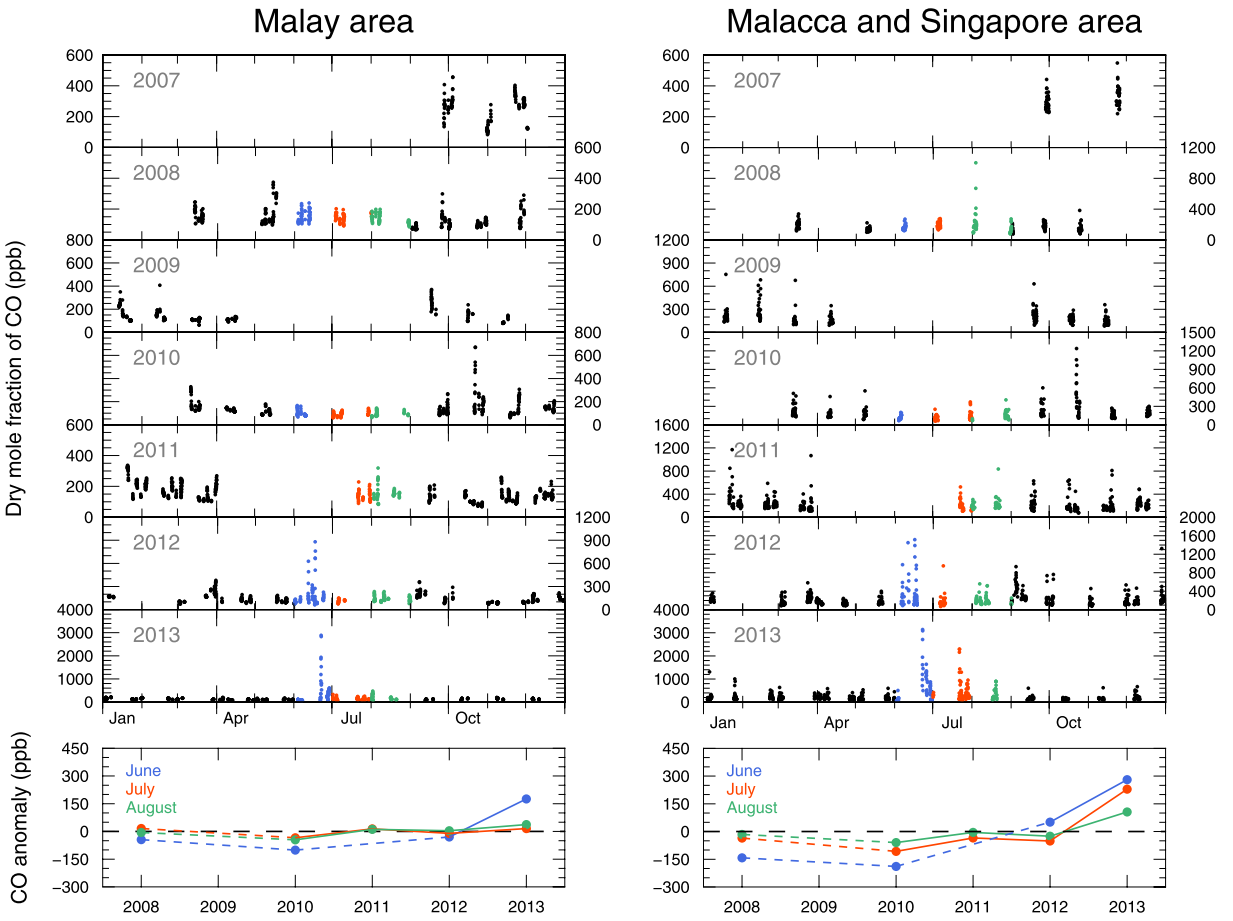

Fig. 3. Temporal variation of the 1-h-mean CO dry mole fractions (upper panels) along with the monthly CO anomaly for June, July and August from 2008 to 2013 (lower panels) observed in the Malay area and the Malacca and Singapore area. The coloured dashed lines in the lower panels represent linear interpolations to account for missing data.

the use of discrete time series data, the VOS observations revealed the general characteristics of the CO distribution and aperiodic CO increases in both areas. In June 2013, an exceptionally high CO level was evident in both the Malay area and the Malacca and Singapore area, and a higher than normal CO level was also observed in the next 2 months in the Malacca and Singapore area.

The impact of these high-CO episodes was clearly illustrated using the monthly CO anomaly, with the anomaly defined as the difference from the 6-year mean CO dry mole fraction observed in these two areas for the corresponding month from 2008 to 2013 (bottom panels of Figure 3). The overall average monthly mean CO values in June, July and August for the 6 years were 199, 127 and 142 ppb, respectively, in the Malay area and 310, 230 and 220 ppb, respectively, in the Malacca and Singapore area. The inter-annual variation in these monthly mean CO values was generally small (i.e. all values are near an anomaly of 0 ppb in the lower panels of Figure 3), but the CO values abruptly increased in 2013. The monthly mean values in June, July and August 2013 for the Malay area were 375, 143 and 179 ppb, respectively, vs. 591, 459 and 326 ppb, respectively, in the Malacca and Singapore area. These results showed large positive CO anomalies only in June for the Malay area and from June to August for the Malacca and Singapore area.

We analyzed the FRP data in the Equatorial Asia region from May to September 2013 by creating gridded FRP data with a spatial resolution of 0.25° × 0.25° from the original satellite hotspot data (Figure 4). Although discrete MODIS FRP observations do not provide continuous FRP emission data, we can use the FRP data to examine the spatial and temporal distribution of active fires and the temporal variation of their fire intensities. The monthly FRP distribution revealed that visible FRP first occurred in north-central Sumatra in June, and subsequently almost disappeared in September after wide spreading of FRP in central Sumatra in August; in contrast, there were few FRPs over the Malaysian Peninsula (Figure 4) and Borneo (data not shown). In particular, most of the high FRP values were found in Riau province in central Sumatra from June to August,

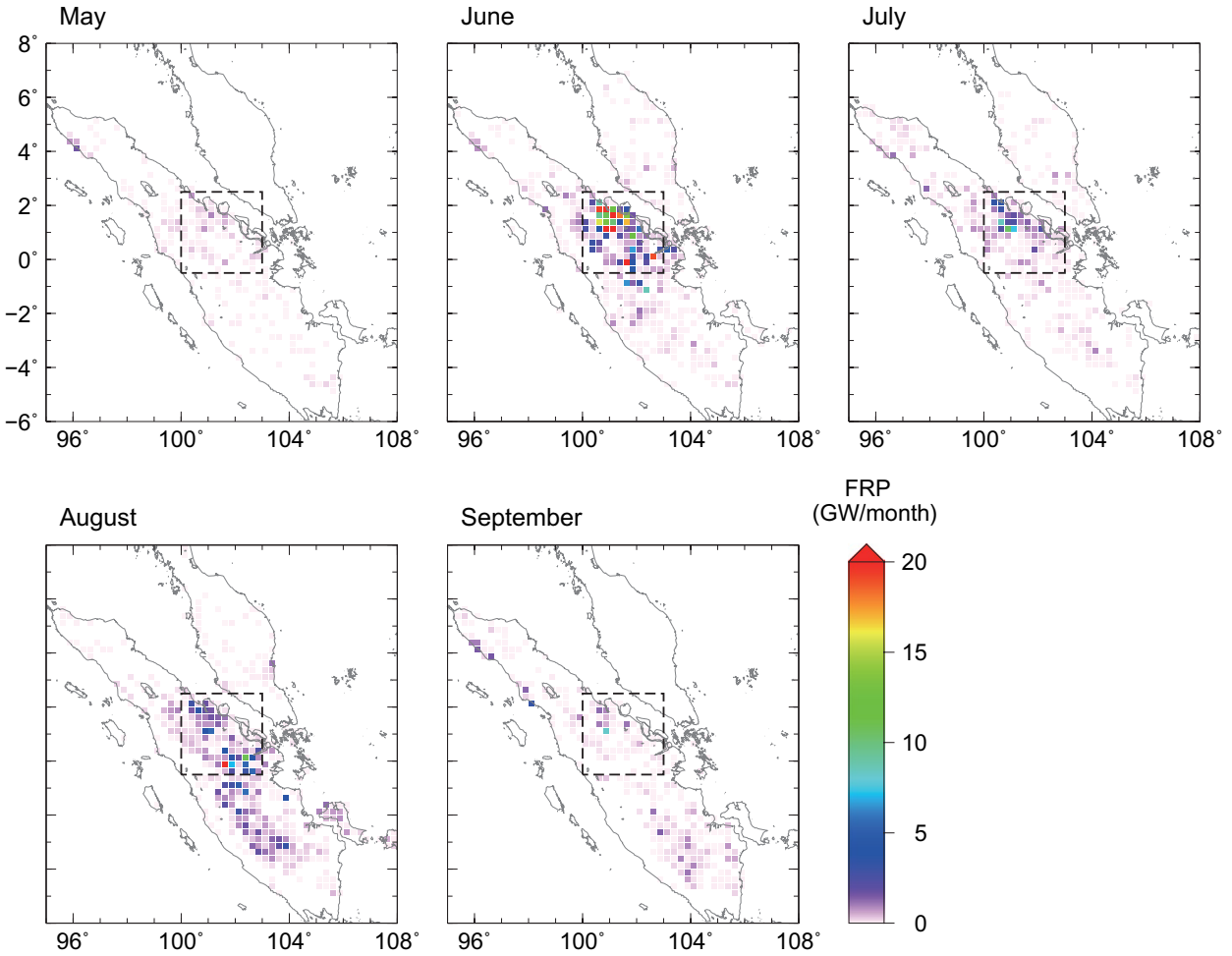

Fig. 4. Distribution of monthly fire radiative power (FRP) intensity with a spatial resolution of 0.25° × 0.25° over Sumatra from May to September 2013. The area over Sumatra surrounded by the dashed square line indicates the study area used for detailed analysis in this study.

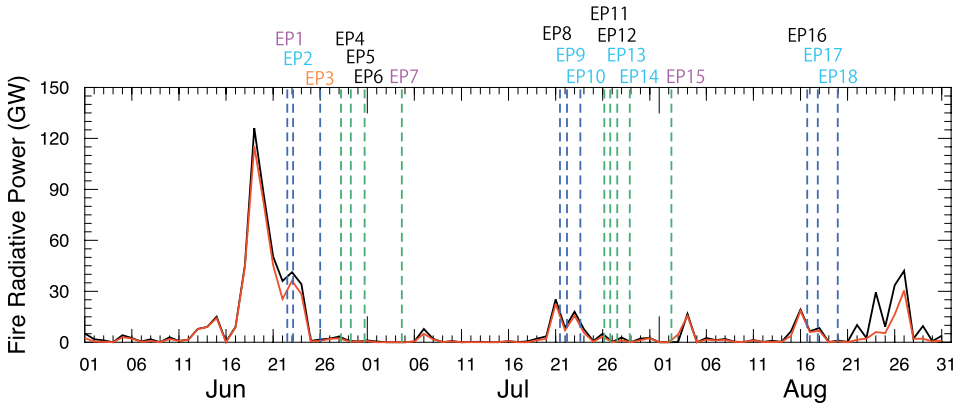

Fig. 5. Time series for the daily FRP value for Sumatra (black line) and the study area (red line) in June, July and August 2013. The vertical dashed lines indicate CO peak times for each CO enhancement episode (shown in Figure 2), using the following colour codes: blue for the *Trans Future 1*, green for the *Fujitrans World*. The colour codes for the episode numbers indicate the estimated transport time for the air masses from the study area to the VOS ship (cyan, up to 1 day; magenta, 2 days; orange, 4 days) based on the backward trajectory analysis; black codes indicate no air mass history that pass directly over the study area. Note that the daily FRP values were derived from discrete MODIS FRP observation.

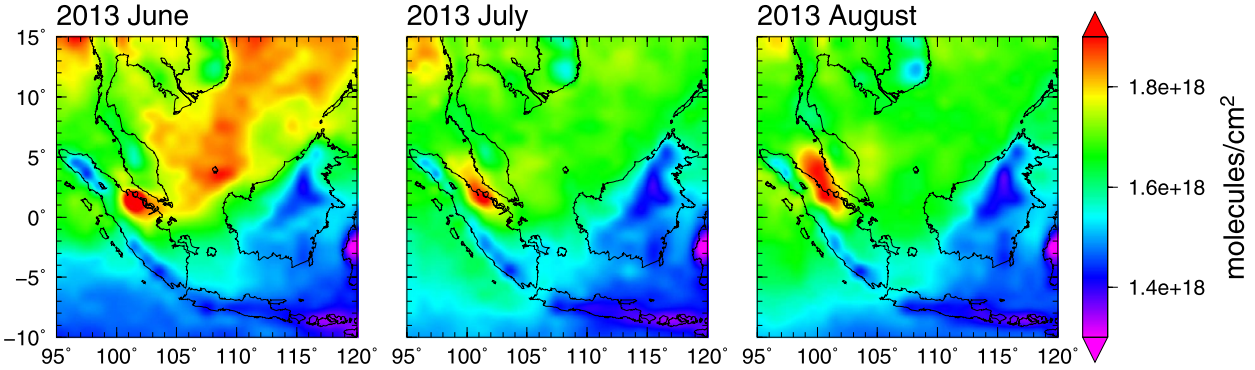

Fig. 6. Monthly column data for the distribution of CO from AIRS data for South-East Asia in June, July and August 2013.

with lower values distributed in central Sumatra in August. Compared to the FRP values in July and August, pronounced FRP values were observed in June, indicating a large temporal variation in the FRP values between June and August.

The time series for the variation of daily FRP values clearly showed high FRP values over Sumatra during the period of only 7 days from 18 to 24 June (Figure 5). Subsequent smaller but relatively high values occurred from 19 to 25 July and from 14 to 19 and 21 to 30 August. These results suggest that biomass burning occurred discontinuously in central Sumatra from June to August 2013, and that the most intense biomass burning occurred in the province of Riau, Sumatra, in June. This is consistent with the report by Gaveau et al. (2014) that a large-scale deforested peatland fire occurred in Riau province in June 2013.

To investigate CO transport from the fire source, we examined the distribution of the CO column concentrations from the AIRS data. The CO column distribution can effectively track the long-range transport of CO from large-scale biomass burning sources (Yurganov et al., 2008; Tanimoto et al., 2009; Nara, Tanimoto, Nojiri, Mukai, Zeng, et al., 2011). On a monthly basis, the AIRS data showed increased CO over north-central Sumatra in June, July and August, and the region of increased CO overlapped with the area with high FRP values (Figure 6). In June, the CO plume stretched from north-central Sumatra to the South China Sea, across the southern part of the Malaysia Peninsula. The CO plume spread over the South China Sea to the north-east, and reached southern China. In contrast, eastward CO transport was weak in July and August, when CO was transported north-westward along the Straits of Malacca. The monthly eastward CO transport in June was successfully tracked by the daily CO column distributions from 17 to 22 June (Figure 7). Although the CO distribution over north-central Sumatra was not clear on 18 and 20 June due to the limited observation coverage, the AIRS still showed a region with elevated CO over north-central Sumatra (17 June) and subsequent formation of a CO plume that expanded from north-central Sumatra to the southern South China Sea, off the western coast

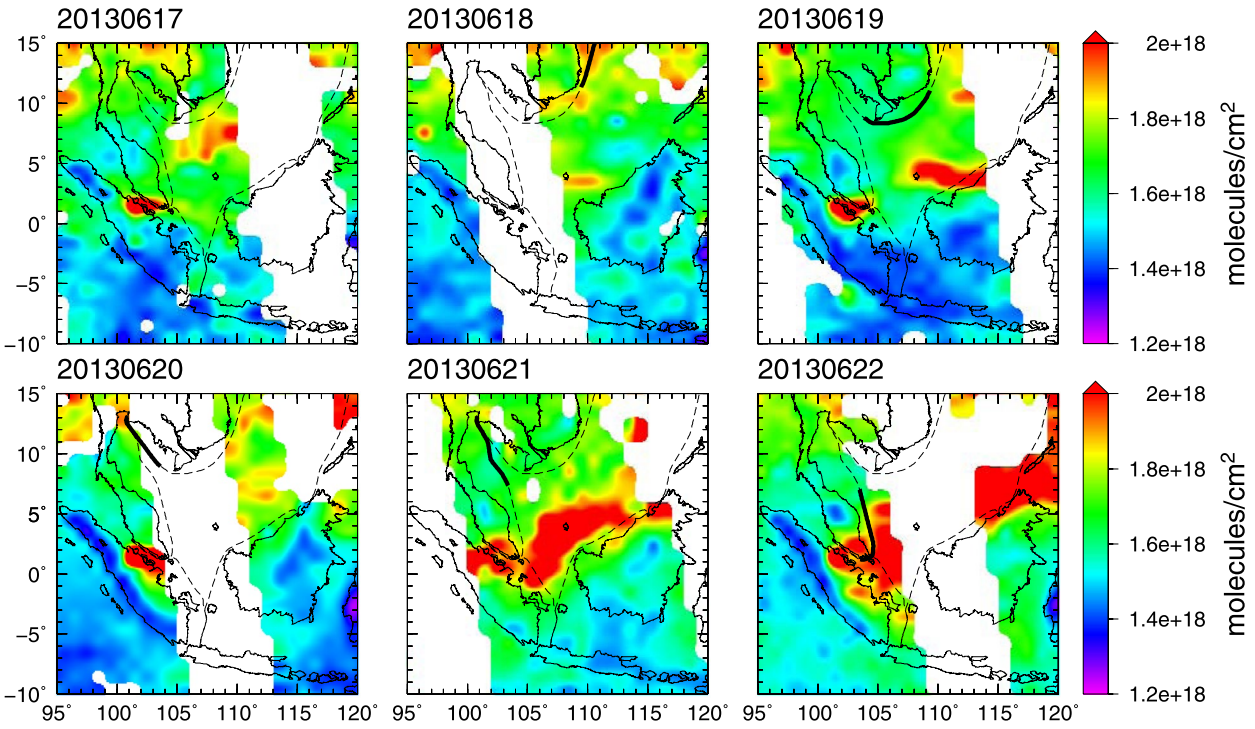

Fig. 7. Daily CO column distribution from the AIRS data for South-East Asia from 17 to 22 June 2013. The ship's route and daily positions are indicated by dashed lines and thick black lines, respectively.

of Borneo (21 June). On 22 June, the CO plume was still clearly visible in the area with satellite coverage, and the VOS ship sailing from Laem Chabang (Thailand) to Port Klang (Malaysia) crossed the CO plume; a large CO increase was observed aboard the ship (EP1 in Figure 2), suggesting that CO transport from north-central Sumatra occurred at surface level.

Overall, analysis of the daily and monthly AIRS data and the shipboard and FRP data suggests that the observed CO enhancements around peninsular Malaysia resulted mainly from the large-scale biomass burning that occurred in north-central Sumatra experiencing anomalously dry conditions despite the absence of El Niño and IOD at this time, and explains the positive CO anomaly that was observed only in June for the Malay area, vs. the anomaly observed in June, July and August in the Malacca and Singapore area.

3.2. *Analysis of fire emissions*

To analyze the fire emissions from the large-scale biomass burning that was responsible for the CO enhancements, we defined a study area between 0.5°S and 2.5°N and between 100°E and 103°E in north-central Sumatra (Figure 4). We compared the time series for overall daily FRP value in the study area with those from Sumatra. The FRP in the study area closely parallels FRP for Sumatra in June and July, although the lines diverge in late August (Figure 5). The monthly total FRP values for Sumatra were approximately 506, 97 and 216 GW in June, July and August, respectively, versus 450, 74 and 128 GW for the study area. The FRP values for the study area therefore accounted for 89% (June), 77% (July) and 59% (August) of the overall Sumatran emission. These results suggest that the fire emission over Sumatra was concentrated in the study area in June and July, whereas the emission outside the study area became much more important in August.

We selected the CO enhancement episodes that were relevant to the analysis of fire emissions from the study area based on the CO dry mole fractions observed during the enhancement episodes, combined with backward trajectory analysis using the CGER/METEX three-dimensional kinematic trajectory model (Zeng et al., 2003). The trajectory calculation was run from the ship's locations where the CO enhancement episode was observed, with an initial trajectory height of 500 m (Figure S-1). We chose four CO enhancement episodes (EP1, EP2, EP3 and EP9) with a particularly large CO increase, in which the mean CO dry mole fraction during the episode was greater than the corresponding monthly mean value calculated above the study area and in which the calculated trajectory from the location representing the CO maximum for each episode passed over the study area during the FRP peak for the study area (Table S-1, Figure 5).

We calculated 10-min mean dry mole fractions for CO_2, CO and CH_4 to scrutinize their variations during the four selected enhancement episodes (Figure 8). During each selected episode,

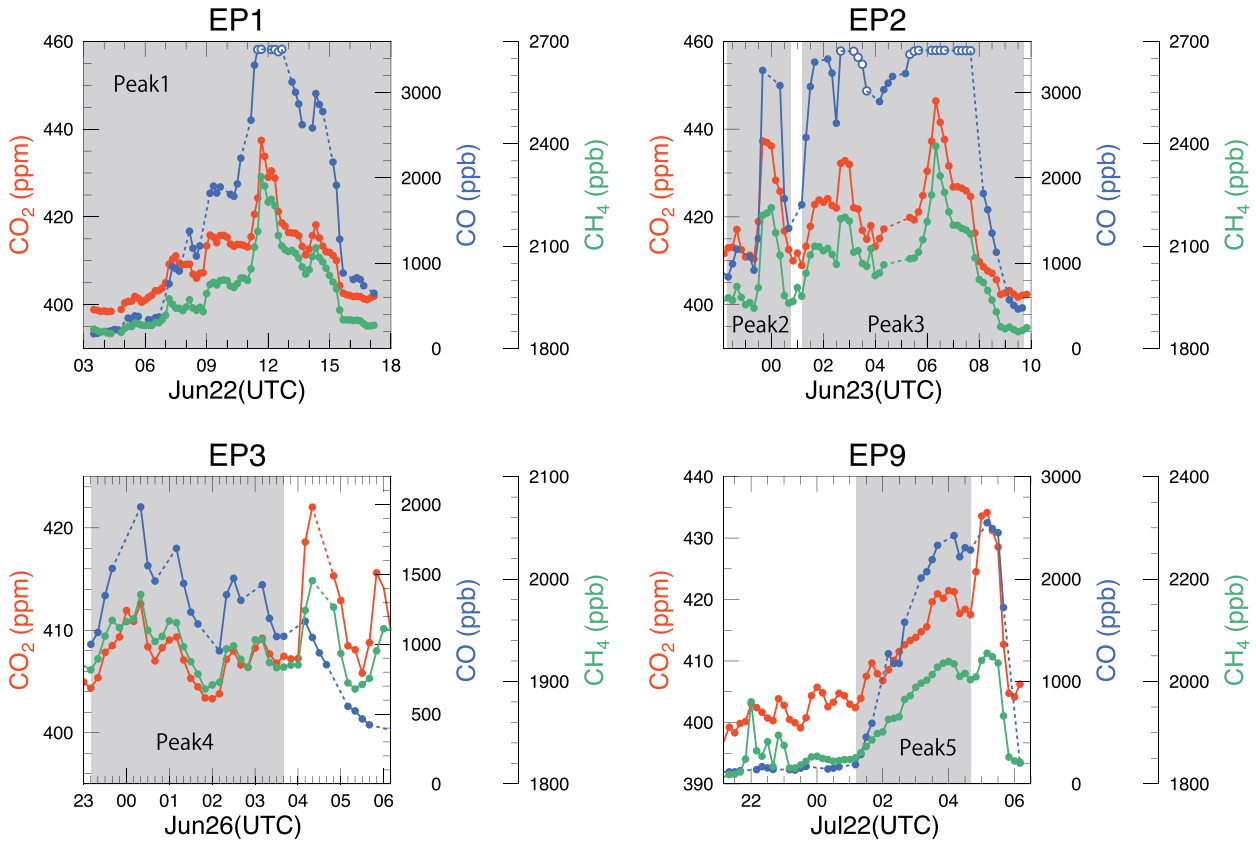

Fig. 8. Temporal variations of the 10-min mean CO_2, CO and CH_4 during the four selected CO enhancement episodes (EP1, EP2, EP3 and EP9). The variations of these gases during the shaded periods were associated with peatland fire emission from the study area, which was identified based on the CO_2-normarized enhancement ratio for CO.

Table 1. Calculated CO_2-normalized enhancement ratios (EnR) for the characterized biomass burning peaks and the estimated average emission factors (EF values) based on the carbon mass balance method and based on GFED4.1s.

			CO_2-normalized EnR (ppb/ppm)		Average EF value (g/kg dry matter)		
	Month	Peak (EP)	CO	CH_4	CO_2	CO	CH_4
Present study	June	Peak 1 (EP1)	150 (9)	12.3 (0.6)	1650 (165)	158 (18)	7.4 (0.8)
		Peak 2 (EP2)	150 (18)	9.2 (0.6)	1654 (165)	158 (17)	5.5 (0.6)
		Peak 3 (EP2)	137 (6)	11.5 (0.4)	1670 (167)	146 (16)	7.0 (0.7)
		Peak 4 (EP3)	127 (12)	10.3 (0.9)	1686 (169)	136 (18)	6.3 (0.8)
	July	Peak 5 (EP9)	137 (8)	10.8 (0.6)	1621 (162)	141 (16)	6.4 (0.7)
GFED4.1s	June		–	–	1676 (18)	156 (38)	13.5 (4.9)
	July		–	–	1666 (18)	133 (34)	10.4 (4.3)

Notes: Numbers in parentheses for the CO_2-normalized EnR denote the standard errors for the reduced major axis regression. For the average EF values, the numbers in parentheses represent the estimated errors propagated from the uncertainty of the carbon content (F_C) and the regression errors for the present study, and represent the standard deviations of the EF values for each grid cell in the study area for GFED4.1s.

the variations in CO_2, CO and CH_4 were generally synchronized and showed several peaks. We examined the emission signatures of these peaks based on the linear relationships between CO_2 and CO, and characterized five peaks relevant to biomass burning with the same fire emission signature (Figure S-2, Table 1). The slope of the linear regression between CO_2 and CO and that between CO_2 and CH_4 during their peak period is defined as the enhancement ratio (EnR), which can be compared directly with the emission ratio because of much shorter transport time of the smoke plumes (<4 days) than the atmospheric lifetimes of CO and CH_4. Especially, the CO_2-normarized EnR of CO from the observations can often be used to assess the contribution of the combustion-related source type responsible for the observed peaks depending on the combustion efficiency.

For example, major biomass burning occurs with a lower combustion efficiency than a fossil fuel combustion, leading to the typical CO/CO_2 values more than 40 ppb/ppm; the typical CO/CO_2 values for tropical forest, savannah, peatland are 89 ± 26, 59 ± 16 and 183 ± 61 ppb/ppm, respectively (Akagi et al., 2011). We calculated the CO_2-normarized EnR of CO using the reduced major axis technique for the characterized five biomass burning peaks. The calculated CO/CO_2 values were higher (127 to 150 ppb/ppm) than the typical CO/CO_2 values for tropical forest and savannah, but lower than that for peatland. These results suggest that peatland fires contributed strongly to the characterized five biomass burning peaks, which is consistent with the report by Gaveau et al. (2014).

Using the calculated CO_2-normalized EnRs for CO along with those corresponding to CH_4, we estimated the average EF values for CO_2, CO and CH_4 individually for the fire emissions from the study area for each of the characterized five biomass burning peaks. EF is defined as the gram amount of a compound emitted per kilogram amount of dry biomass burned, expressed by the carbon mass balance method (Ward and Radke, 1993; Yokelson et al., 1999):

$$\mathrm{EF}_n = F_c \times 1000 \times \frac{\mathrm{MW}_n}{\mathrm{AW}_C} \times \left\{ \frac{\mathrm{EnR}_n}{1 + \mathrm{EnR}_{\mathrm{CO}} + \mathrm{EnR}_{\mathrm{CH4}} + \mathrm{EnR}_{\mathrm{VOCs}} + \mathrm{EnR}_{\mathrm{aerosols}}} \right\}, \quad (1)$$

where EF_n is the emission factor for substance n, F_C is the carbon content (by mass) in the fuel, MW_n is the molecular weight of compound n, AW_C is the atomic weight of carbon and EnR is the CO_2-normalized EnR for the subscripted compound (n, CO, CH_4, VOCs, aerosols), where VOCs and aerosols represent the sum of the EnR values for individual volatile organic compounds and carbon-containing aerosol species, respectively. The carbon mass balance method is based on the idea that the fuel carbon burned in a fire is completely converted into the form of carbon-containing species: CO_2, CO, CH_4, VOCs and aerosols, and then all of that substance is released into the atmosphere. Although we did not measure individual VOCs and aerosols, the total carbon from a fire can be approximated as the sum of the observed CO_2, CO and CH_4 because these substances comprise more than 95% of the total carbon mass emitted by a fire, even for smouldering combustion of peat soils (Akagi et al., 2011; Stockwell et al., 2014). Thus, our estimated emission factors include a possible overestimation of 5%.

We computed the average F_C used in Equation (1) for the combusted biomass in the study area for June and July 2013 using GFED4.1s. In each grid cell of GFED4.1s with a spatial resolution of 0.25° × 0.25°, we first calculated the average F_C value by averaging the default F_C value assigned for each fuel type, weighted by the fractional contribution of these different fire types in the cell; the assigned F_C values were 0.44 for agricultural waste burning, 0.56 for peat fires, 0.48 for grassland and savannah fires and 0.48 for tropical forest fires in areas of deforestation and degradation (van der Werf et al., 2010). Subsequently, we calculated the overall average F_C values in the study area, weighted by the dry matter emission in each cell of the grid. From these calculations, we estimated an overall average F_C value of 0.523 for June and 0.514 for July, with a conservative uncertainty of ±10% for the EF estimation. Table 1 summarizes the estimated average EF values for CO_2, CO and CH_4.

We compared the estimated average EF values with the monthly average EF values for fire emissions from the study area based on GFED4.1s using the recommended EFs (Table 1). Despite the wide variability among the EF values used in GFED4.1s, the estimated average EF values for CO agreed well with those predicted by GFED4.1s as well as CO_2. However, for CH_4, the estimated average EF was substantially lower than that in GFED4.1s. The fire types involving the fire emissions from the study area in GFED4.1s are agricultural waste burning, peat fires, grassland and savannah fires, and tropical forest fires in areas of deforestation and degradation; these have EF values of 5.82, 20.8, 1.94 and 5.07, respectively, for CH_4. Because only the peat fires had a much higher EF (20.8) than the estimated average EF values in the present study (5.5 to 7.4 in Table 1), the higher average EF values from GFED4.1s (13.5 for June

Table 2. Estimated optimal emission factors (EF values) for the peat used in GFED4.1s, and values reported in past studies.

	Study area/sample	Peak (present study)/no. samples (previous studies)	EF of peat (g/kg dry matter)		
			CO_2	CO	CH_4
Present study	North-central Sumatra	Peak 1 (EP1)	1656	213	9.4
		Peak 2 (EP2)	1664	214	6.0
		Peak 3 (EP2)	1692	191	6.0
		Peak 4 (EP3)	1723	174	7.4
		Peak 5 (EP9)	1579	235	9.0
		Average (SD)	1663 (54)	205 (23)	7.6 (1.6)
Christian et al. (2003)	South Sumatra peat	1	1703	210.3	20.8
Huijnen et al. (2016)	South Borneo	11	1594 (61)	255 (39)	7.4 (2.3)
Stockwell et al. (2016)	South Borneo	35	1564 (77)	291 (49)	9.51 (4.74)

Notes: Numbers in parentheses for the EF values in the present study represent the standard deviation of the five optimal EF values; those for Huijnen et al. (2016) and Stockwell et al. (2016) are the standard deviation of the EF values based on their observations.

and 10.4 for July) than those from the present study can be explained only by the contribution of peat fires, suggesting an overestimation of the CH_4 EF for peat fires. Although the EF values recommended for use in GFED4.1s were compiled from several past studies, the value for peat fires was derived from a single study by Christian et al. (2003) that reported the EF for the Sumatra peat based on a single laboratory combustion experiment using a peat soil sample collected from south Sumatra. The present results suggest a high uncertainty in the EF of CH_4 for peat fires, even though GFED4.1s reproduced the fire emissions for CO_2 and CO well in the study area.

3.3. *Estimation of the typical EF for peat fires*

We estimated the optimal EF values of CO_2, CO and CH_4 for the peat fires based on the estimated average EF values for each selected biomass burning peak so that the average EF values in the study area predicted by GFED4.1s matched those from our observations, while retaining the original EF values for agricultural waste burning, grassland and savannah fires, and tropical forest fires in areas of deforestation and degradation (Table 2). We averaged the estimated optimal EF values for CO_2, CO and CH_4 individually to determine their typical EF values for peat fires. As expected, the typical EF values for CO_2 and CO agreed well with GFED4.1s-recommended EF values from Christian et al. (2003), whereas our typical EF for CH_4 was substantially lower than the GFED4.1s-recommended value. We assessed the typical EF values by comparing the fire emissions estimates from north-central Sumatra based on GFED4.1s with those from a previous study (Gaveau et al., 2014) (Table 3). Gaveau et al. (2014) estimated the fire emissions from the Riau province based on LANDSAT satellite imagery, validated with visual observations using an unmanned aerial vehicle. Owing to the similar spatial coverage of the study areas between our study and Gaveau et al. (2014) where intense biomass burning occurred, GFED4.1s using the recommended EF values provided fire emissions estimates which fell within 20% (+11% for CO_2, −11% for CO, −20% for CH_4) of those from Gaveau et al. (2014). By applying the typical EF values, the fire emissions estimate for CH_4 decreased to about 40% of that from Gaveau et al. (2014), whereas there was little change for CO_2 and CO. This lower estimate for CH_4 is due likely to application of the GFED4.1s-recommended EF for peat fires in the estimates by Gaveau et al. (2014). These results suggest that GFED4.1s provides reasonable fire carbon estimates for the Sumatran peatland fires but that the current EF of CH_4 for peat fires was greatly overestimated.

Table 3. Estimated fire emission of CO_2, CO and CH_4 from the study area in June based on GFED4.1s using the estimated typical and the GFED4.1s-recommended emission factors for peat fires, and the emission estimates from a previous study.

Method	EF values for peat fires	CO_2 (Tg)	CO (Tg)	CH_4 (Tg)
GFED4.1s	Present study	106.12	9.83	0.41
	GFED4.1s-recommended	105.03	9.76	0.85
Gaveau et al. (2014)	GFED4.1s-recommended	94.84 ± 44.42	10.98 ± 5.47	1.06 ± 0.54

Two recent studies based on independent observations reported EF values of CH_4 for peat fires similar to the estimated typical EF as listed in Table 2 (Huijnen et al., 2016; Stockwell et al., 2016). These studies estimated the EF values for CO_2, CO and CH_4 for Borneo peat through *in situ* measurements of a number of smoke plumes from smouldering peat fires observed near Palangkaraya, south of Borneo's Central Kalimantan Province, late in the fire season of 2015. The EF values for CH_4 from these two studies agreed well with the typical EF in the present study, and all three EF values were less than half of the recommended EF in GFED4.1s (Table 2). In contrast, we found no clear difference in the EF values for CO_2 and CO among the estimated EF values due to the large variability in these estimates, whereas the EF values from the two observation-based studies showed more reduced values (i.e. lower CO_2 with higher CO) than the recommended EF values. These results strongly support the overestimation of the CH_4 EF for peat fires in GFED4.1s, probably by more than a factor of two, and suggest the need for further investigation to characterize the EF values for CO_2 and CO.

Another constraint can be obtained from Worden et al. (2013). These investigators estimated the CH_4 emissions from large-scale Indonesian fires that occurred in 2006 using satellite observation data and GEOS-Chem model simulation. The estimated CH_4 emissions were compared with the a priori fire emissions estimates based on GFED2 that used the CH_4 EF for peat fires represented by the value for tropical forest fires (6.8 g/kg dry matter) from Andreae and Merlet (2001) owing to lack of information on peat fires (van der Werf et al., 2006). Despite that the CH_4 EF is about one-third of that used in the current GFED4s (20.8 g/kg dry matter), Worden et al. (2013) showed a good agreement between their estimate and the a priori estimate based on GFED2. Nara, Tanimoto, Nojiri, Mukai, Zeng, et al., 2011 reported a large contribution of peatland fires to the Indonesian fires in 2006 based on the shipboard observation; consequently, this agreement indicates an overestimation of CH_4 emissions from peatland fires when applying the CH_4 EF from GFED4.1s. Our estimated typical CH_4 EF is comparable with that from GFED2, and consistent with the emission estimate by Worden et al. (2013).

According to van der Werf et al. (2010), the average contribution of Equatorial Asia to global fire emissions of CH_4 from 1997 to 2009 was high, amounting to 32% of the total, mainly due to the high EF for peat. However, the substantial improvement of the CH_4 EF value for peat fires in the present study can result in a decreased estimate of the regional contribution to global CH_4 fire emission compared with current estimates, especially in drought years.

4. Summary and conclusions

We observed simultaneous enhancements of CO_2, CO and CH_4 around the Malay Peninsula in South-East Asia from June to August 2013 using systematic shipboard observations. We detected 18 episodes of CO enhancement which showed the most prominent enhancement among the observed gases during the study period. The area mean for the monthly dry mole fraction of CO was largest in June, followed by July and August, in the Malacca and Singapore area, but a significant increase was only observed in June in the Malay area. These CO enhancement episodes were responsible for the largest positive anomaly of CO in June, July and August 2013 in each area based on the shipboard observations from 2007 to 2013. The satellite data revealed that the observed CO enhancements were mainly associated with intense large-scale biomass burning in Riau province in Sumatra. From the 18 observed episodes of CO enhancement, we selected four episodes associated with fire emissions from north-central Sumatra based on the mean dry mole fraction of CO during the episode and backward trajectory analysis, and identified five biomass burning peaks that involved peatland fires based on the CO_2-normalized enhancement ratio of CO.

From the calculated CO_2-normalized enhancement ratio for CO and CH_4 for the five biomass burning peaks, we estimated the average EF values for CO_2, CO and CH_4 for the study area where intense FRP emissions were observed. The average EF values estimated in the present study were in good agreement with those predicted by GFED4.1s for CO_2 and CO using GFED4.1s-recommended EF values, but differed greatly for CH_4, suggesting a large uncertainty in the recommended CH_4 EF for peat fires. We determined typical EF values for peat fires using the average EF values from the present study, resulting in EF values of 1663 ± 54, 205 ± 23 and 7.6 ± 1.6 g/kg dry matter for CO_2, CO and CH_4, respectively. Whereas the large variability among the estimated EF values for CO_2 and CO indicates a need for further investigation to determine their typical EF values for peat fires, the typical CH_4 EF was consistent with the EF values for peat fires reported by previous researchers, at less than half of the current GFED4.1s-recommended EF for CH_4. These results suggest the overestimation of the EF value of CH_4 for peat fires in GFED4.1s. Improving the CH_4 EF value for peat fires can greatly decrease the contribution of Equatorial Asia to the global emission of CH_4 from fires using GFED4.1s, especially in drought years.

Acknowledgements

We are grateful to the Toyofuji Shipping Co., Ltd and Kagoshima Senpaku Kaisha, Ltd. for their generous cooperation and participation in the NIES-VOS program. We thank S. Kariya and T. Yamada of the Global Environmental Forum for their assistance with data collection during the NIES-VOS program and C. Wada of NIES for primary data processing. We also thank E. T. Nagy for supporting the proofreading. We are thankful to two anonymous reviewers for careful reading and useful comments.

Disclosure statement

No potential conflict of interest was reported by the authors.

Funding

This research was supported by the Global Environment Research Account for National Institutes by the Ministry of the Environment, Japan [grant number E1253].

Supplemental data

Supplemental data for this article can be accessed here https://doi.org/10.1080/16000889.2017.1399047.

References

Akagi, S. K., Yokelson, R. J., Wiedinmyer, C., Alvarado, M. J., Reid, J. S. and co-authors. 2011. Emission factors for open and domestic biomass burning for use in atmospheric models. *Atmos. Chem. Phys.* **11**, 4039–4072. DOI:10.5194/acp-11-4039-2011.

Andela, N., Morton, D. C., Giglio, L., Chen, Y., van der Werf, G. R. and co-authors. 2017. A human-driven decline in global burned area. *Science* **356**, 1356–1362. DOI:10.1126/science.aal4108.

Andreae, M. O. and Merlet, P. 2001. Emission of trace gases and aerosols from biomass burning. *Glob. Biogeochem. Cycles* **15**, 955–966. DOI:10.1029/2000GB001382.

Aumann, H. H., Chahine, M. T., Gautier, C., Goldberg, M., Kalnay, E. and co-authors. 2003. AIRS/AMSU/HSB on the aqua mission: design, science objectives, data products, and processing systems. *IEEE Trans. Geosci. Remote Sens.* **41**, 253–264.

Bond, W. J. and Keeley, J. E. 2005. Fire as a global 'herbivore': the ecology and evolution of flammable ecosystems. *Trends Ecol. Evol.* **20**, 387–394.

Chandra, S., Ziemke, J. R., Duncan, B. N., Diehl, T. L., Livesey, N. J. and co-authors. 2009. Effects of the 2006 El Niño on tropospheric ozone and carbon monoxide: implications for dynamics and biomass burning. *Atmos. Chem. Phys.* **9**, 4239–4249. DOI:10.5194/acp-9-4239-2009.

Christian, T. J., Kleiss, B., Yokelson, R. J., Holzinger, R., Crutzen, P. J. and co-authors. 2003. Comprehensive laboratory measurements of biomass-burning emissions: 1. Emissions from Indonesian, African, and other fuels. *J. Geophys. Res.* **108**. 4719. DOI:10.1029/2003JD003704.

Crutzen, P. J. and Andreae, M. O. 1990. Biomass burning in the tropics: impact on atmospheric chemistry and biogeochemical cycles. *Science* **250**, 1669–1678.

Field, R. D. and Shen, S. S. P. 2008. Predictability of carbon emissions from biomass burning in Indonesia from 1997 to 2006. *J. Geophys. Res.* **113**. G04024. DOI:10.1029/2008JG000694.

Field, R. D., van der Werf, G. R. and Shen, S. S. P. 2009. Human amplification of drought-induced biomass burning in Indonesia since 1960. *Nat. Geosci.* **2**, 185–188.

Friedl, M. A., Sulla-Menashe, D., Tan, B., Schneider, A., Ramankutty, N. and co-authors. 2010. MODIS collection 5 global land cover: algorithm refinements and characterization of new datasets. *Rem. Sens. Environ.* **114**, 168–182. DOI:10.1016/j.rse.2009.08.016.

Gaveau, D. L. A., Salim, M. A., Hergoualc'h, K., Locatelli, B., Sloan, S. and co-authors. 2014. Major atmospheric emissions from peat fires in Southeast Asia during non-drought years: evidence from the 2013 Sumatran fires. *Sci. Rep.* **4**, 1–7. DOI:10.1038/srep06112.

Giglio, L., Csiszar, I. and Justice, C. O. 2006. Global distribution and seasonality of active fires as observed with the Terra and Aqua Moderate Resolution Imaging Spectroradiometer (MODIS) sensors. *J. Geophys. Res.* **111**, G02016. DOI:10.1029/2005JG000142.

Giglio, L., Descloitres, J., Justice, C. O. and Kaufman, Y. 2003. An enhanced contextual fire detection algorithm for MODIS. *Remote Sens. Environ.* **87**, 273–282.

Giglio, L., Loboda, T., Roy, D. P., Quayle, B. and Justice, C. O. 2009. An active-fire based burned area mapping algorithm for the MODIS sensor. *Remote Sens. Environ.* **113**, 408–420.

Giglio, L., Randerson, J. T. and van der Werf, G. R. 2013. Analysis of daily, monthly, and annual burned area using the fourth-generation global fire emissions database (GFED4). *J. Geophys. Res.* **118**, 317–328. DOI:10.1002/jgrg.20042.

Huijnen, V., Wooster, M. J., Kaiser, J. W., Gaveau, D. L. A., Flemming, J. and co-authors. 2016. Fire carbon emissions over maritime southeast Asia in 2015 largest since 1997. Sci. Rep. **6**, 26886. DOI:10.1038/srep26886.

Ichoku, C., Giglio, L., Wooster, M. J. and Remer, L. A. 2008. Global characterization of biomass-burning patterns using satellite measurements of fire radiative energy. *Remote Sens. Environ.* **112**, 2950–2962.

Kaufman, Y. J., Justice, C. O., Flynn, L. P., Kendall, J. D., Prins, E. M. and co-authors. 1998. Potential global fire monitoring from EOS-MODIS. *J. Geophys. Res.* **103**, 32215–32238.

Langenfelds, R. L., Francey, R. J., Pak, B. C., Steele, L. P., Lloyd, J. and co-authors. 2002. Interannual growth rate variations of atmospheric CO2 and its $\delta^{13}C$, H_2, CH_4, and CO between 1992 and 1999 linked to biomass burning. *Global Biogeochem. Cycles* **16**, 1048. DOI:10.1029/2001GB001466.

Logan, J. A., Megretskaia, I., Nassar, R., Murray, L. T., Zhang, L. and co-authors. 2008. Effects of the 2006 El Niño on tropospheric composition as revealed by data from the Tropospheric Emission Spectrometer (TES). *Geophys. Res. Lett.* **35**, L03816. DOI:10.1029/2007/GL031698.

Margono, B. A., Potapov, P. V., Turubanova, S. T., Stolle, F. and Hansen, M. C. 2014. Primary forest cover loss in Indonesia over 2000–2012. *Nat. Clim. Change* **4**, 730–735. DOI:10.1038/nclimate2277.

Marlier, M. E., Defries, R. S., Voulgarakis, A., Kinney, P. L., Randerson, J. T. and co-authors. 2013. El Niño and health risks from landscape fire emissions in southeast Asia. *Nat. Clim. Change* **3**, 131–136. DOI:10.1038/nclimate1658.

Marlon, J. R., Bartlein, P. J., Carcaillet, C., Gavin, D. G., Harrison, S. P. and co-authors. 2009. Climate and human influences on global biomass burning over the past two millennia. *Nat. Geosci.* **1**, 697–701. DOI:10.1038/ngeo313.

McMillan, W. W., Barnet, C., Strow, L., Chahine, M., Warner, J. and co-authors. 2005. Daily global maps of carbon monoxide from NASA's atmospheric infrared sounder. *Geophys. Res. Lett.* **32**, L11801. DOI:10.1029/2004GL021821.

McMillan, W. W., Evans, K. D., Barnet, C. D., Maddy, E. S., Sachse, G. W. and co-authors. 2011. AIRS V5 CO retrieval with DACOM *in situ* measurements. *IEEE T Geosci. Remote.* **49**, 1–12. ISSN:0196-2892. DOI:10.1109/TGRS.2011.2106505.

Miettinen, J., Hooijer, A., Shi, C., Tollenaar, D., Vernimmen, R. and co-authors. 2012. Extent of industrial plantations on Southeast Asian peatlands in 2010 with analysis of historical expansion and future projections. *Global Change Boil. Bioenergy* **4**, 908–918. DOI:10.1111/j.1757-1707.2012.01172.x.

Miettinen, J., Hooijer, A., Wang, J., Shi, C. and Liew, S. C. 2012. Peatland degradation and conversion sequences and interrelations in Sumatra. *Reg. Environ. Change* **12**, 729–737. DOI:10.1007/s10113-012-0290-9.

Miettinen, J., Shi, C. and Liew, S. C. 2011. Influence of peatland and land cover distribution on fire regimes in insular Southeast Asia. *Reg. Environ. Change* **11**, 191–201. DOI:10.1007/s10113-010-0131-7.

Miettinen, J., Shi, C. and Liew, S. C. 2012. Two decades of destruction in Southeast Asia's peat swamp forests. *Front. Ecol. Environ.* **10**, 124–128. DOI:10.1890/100236.

Miettinen, J., Shi, C. and Liew, S. C. 2016. Land cover distribution in the peatlands of Peninsular Malaysia, Sumatra and Borneo in 2015 with changes since 1990. *Global Ecology and Conservation* **6**, 67–78.

Nara, H., Tanimoto, H., Nojiri, Y., Mukai, H., Machida, T. and co-authors. 2011. Onboard measurement system of atmospheric carbon monoxide in the Pacific by voluntary observing ships. *Atmos. Meas. Tech.* **4**, 2495–2507. DOI:10.5194/amt-4-2495-2011.

Nara, H., Tanimoto, H., Nojiri, Y., Mukai, H., Zeng, J. and co-authors. 2011. CO emissions from biomass burning in South-east Asia in the 2006 El Niño year: shipboard and AIRS satellite observations. *Environ. Chem.* **8**, 213–223. DOI:10.1071/EN10113.

Nara, H., Tanimoto, H., Tohjima, Y., Mukai, H., Nojiri, Y. and co-authors. 2014. Emissions of methane from offshore oil and gas platforms in Southeast Asia. *Sci. Rep.* **4**, 6503. DOI:10.1038/srep06503.

Page, S. E., Siegert, F., Rieley, J. O., Boehm, H.-D. V., Jaya, A. and co-authors. 2002. The amount of carbon released from peat and forest fires in Indonesia during 1997. *Nature* **420**, 61–65.

Randerson, J. T., Chen, Y., van der Werf, G. R., Rogers, B. M. and Morton, D. C. 2012. Global burned area and biomass burning emissions from small fires. *J. Geophys. Res.* **117**, G04012. DOI:10.1029/2012JG002128.

Schultz, M. G., Heil, A., Hoelzemann, J. J., Spessa, A., Thonicke, K. and co-authors. 2008. Global wildland fire emissions from 1960 to 2000. Global Biogechem. Cycles **22**, GB2002. DOI:10.1029/2007GB003031.

Siegert, F., Ruecker, G., Hinrichs, A. and Hoffmann, A. A. 2001. Increased damage from fires in logged forests during droughts caused by El Niño. *Nature* **414**, 437–440.

Stockwell, C. E., Jayarathne, T., Cochrane, M. A., Ryan, K. C., Putra, E. I. and co-authors. 2016. Field measurements of trace gases and aerosols emitted by peat fires in Central Kalimantan, Indonesia, during the 2015 El Niño. *Atmos. Chem. Phys.* **16**, 11711–11732. DOI:10.5194/acp-16-11711-2016.

Stockwell, C. E., Yokelson, R. J., Kreidenweis, S. M., Robinson, A. L., DeMott, P. J. and co-authors. 2014. Trace gas emissions from combustion of peat, crop residue, domestic biofuels, grasses, and other fuels: configuration and Fourier transform infrared (FTIR) component of the fourth Fire Lab at Missoula Experiment (FLAME-4). *Atmos. Chem. Phys.* **14**, 9727–9754. DOI:10.5194/acp-14-9727-2014.

Susskind, J., Barnet, C. D. and Blaisdell, J. M. 2003. Retrieval of atmospheric and surface parameters from AIRS/AMSU/HSB data in the presence of clouds. *IEEE Trans. Geosci. Remote Sens.* **41**, 390–409.

Susskind, J., Blaisdell, J. M., Iredell, L. and Keita, F. 2011. Improved temperature sounding and quality control methodology using AIRS/AMSU data: the AIRS science team version 5 retrieval algorithm. *IEEE Trans. Geosci. Remote Sens.* **49**, 883–907.

Tanimoto, H., Sato, K., Butler, T., Lawrence, M. G., Fisher, J. A. and co-authors. 2009. Exploring CO pollution episodes observed at Rishiri Island by chemical weather simulations and AIRS satellite measurements: long-range transport of burning plumes and implications for emissions inventories. *Tellus* **61B**, 394–407.

Terao, Y., Mukai, H., Nojiri, Y., Machida, T., Tohjima, Y. and co-authors. 2011. Interannual variability and trends in atmospheric methane over the western Pacific from 1994 to 2010. *J. Geophys. Res.* **116**, 439. DOI:10.1029/2010JD015467.

Tohjima, Y., Minejima, C., Mukai, H., Machida, T., Yamagishi, H. and co-authors. 2012. Analysis of seasonality and annual mean distribution of atmospheric potential oxygen (APO) in the Pacific region. Global Biogeochem. Cycles **26**, GB4008. DOI:10.1029/2011GB004110.

Tohjima, Y., Terao, Y., Mukai, H., MacHida, T., Nojiri, Y. and co-authors. 2015. ENSO-related variability in latitudinal distribution of annual mean atmospheric potential oxygen (APO) in the equatorial Western Pacific. *Tellus* **67**, 25869. DOI:10.3402/tellusb.v67.25869.

Wang, Z., Chappellaz, J., Park, K. and Mak, J. E. 2010. Large variations in southern hemisphere biomass burning during the last 650 years. *Science* **330**, 1663–1666. DOI:10.1126/science.1197257.

Ward, D. E. and Radke, L. F. 1993. Emissions measurements from vegetation fires: a comparative evaluation of methods and results. In: *Fire in the Environment: The Ecological, Atmospheric and Climatic Importance of Vegetation Fires* (eds. P. J. Crutzen and J. G. Goldammer). Wiley, New York, NY, pp. 53–76.

van der Werf, G. R., Dempewolf, J., Trigg, S. N., Randerson, J. T., Kasibhatla, P. S. and co-authors. 2008. Climate regulation of fire emissions and deforestation in equatorial Asia. *P. Nat. Acad. Sci. USA* **105**, 20350–20355. DOI:10.1073/pnas.0803375105.

van der Werf, G. R., Randerson, J. T., Collatz, G. J., Giglio, L., Kasibhatla, P. S. and co-authors. 2004. Continental-scale partitioning of fire emissions during the 1997 to 2001 El Niño/La Niña period. *Science* **303**, 73–76.

van der Werf, G. R., Randerson, J. T., Giglio, L., Collatz, G. J., Kasibhatla, P. S. and co-authors, 2006. Interannual variability in global biomass burning emissions from 1997 to 2004. *Atmos. Chem. Phys.* **6**, 3423–3441.

van der Werf, G. R., Randerson, J. T., Giglio, L., Collatz, G. J., Mu, M. and co-authors 2010. Global fire emissions and the contribution of deforestation, savanna, forest, agricultural, and peat fires (1997–2009). *Atmos. Chem. Phys.* **10**, 11707–11735. DOI:10.5194/acp-10-11707-2010.

Wooster, M. J. 2002. Small-scale experimental testing of fire radiative energy for quantifying mass combusted in natural vegetation fires. *Geophys. Res. Lett.* **29**, 5. DOI:10.1029/2002GL015487.

Wooster, M. J., Roberts, G., Perry, G. L. W. and Kaufman, Y. J. 2005. Retrieval of biomass combustion rates and totals from fire radiative power observations: FRP derivation and calibration relationships between biomass consumption and fire radiative energy release. *J. Geophys. Res.* **110**, D24311. DOI:10.1029/2005JD006318.

Worden, J., Jiang, Z., Jones, D. B. A., Alvarado, M., Bowman, K. and co-authors. 2013. El Niño, the 2006 Indonesian peat fires, and the distribution of atmospheric methane. *Geophys. Res. Lett.* **40**, 1–6. DOI:10.1002/grl.50937.

Yokelson, R. J., Goode, J. G., Ward, D. E., Susott, R. A., Babbitt, R. E. and co-authors. 1999. Emissions of formaldehyde, acetic acid, methanol, and other trace gases from biomass fires in North Carolina measured by airborne Fourier transform infrared spectroscopy. *J. Geophys. Res.* **104**, 30109–30125. DOI:10.1029/1999JD900817.

Yokelson, R. J., Susott, R., Ward, D. E., Reardon, J. and Griffith, D. W. T. 1997. Emissions from smoldering combustion of biomass measured by open-path Fourier transform infrared spectroscopy. *J. Geopyhs. Res.* **102**, 18865–18877.

Yurganov, L. N., McMillan, W. W., Dzhola, A. V., Grechko, E. I., Jones, N. B. and co-authors. 2008. Global AIRS and MOPITT CO measurements: Validation, comparison, and links to biomass burning variations and carbon cycle. *J. Geophys. Res.* **113**, D09301. DOI:10.1029/2007JD009229.

Zeng, N., Mariotti, A. and Wetzel, P. 2005. Terrestrial mechanisms of interannual CO_2 variability. *Global Biogeochem. Cycles* **19**, GB1016. DOI:10.1029/2004GB002273.

Zeng, J., Tohjima, Y., Fujinuma, Y., Mukai, H. and Katsumoto, M. 2003. A study of trajectory quality using methane measurements from Hateruma Island. *Atmos. Environ.* **37**, 1911–1919. DOI:10.1016/S1352-2310(03)00048-7.